10670 *Inorg. Chem.* **2009**, *48*, 10670–10678
DOI: 10.1021/ic901372k

Inorganic Chemistry
Article

Multiple Folding Structures Mediated by Metal Coordination of Acyclic Multidentate Ligand

Shigehisa Akine, Yoko Morita, Fumihiko Utsuno, and Tatsuya Nabeshima*

Graduate School of Pure and Applied Sciences, University of Tsukuba, Tsukuba, Ibaraki 305-8571, Japan

Received July 13, 2009

Four kinds of folded structures are formed upon the metal complexation of a bis(N_2O_2) ligand in which two oxime-type N_2O_2 chelate ligands are connected by a flexible diethyleneoxy linker. The N_2O_2 coordination sites are intended for d-block transition-metal ions, and the diethyleneoxy linker can interact with hard metal cations. Meso double helical, folded Ω-shaped, S-shaped helical, and single helical structures were formed depending on the metal combination. The difference in the affinity to metal cations resulted in variation of the folding modes and enabled the structural conversion between the folded structures.

Introduction

Foldamers are discrete chain molecules or oligomers that can spontaneously form well-defined higher-order structures such as helical structures.[1] These higher-order structures are maintained by relatively weak noncovalent interactions. Based on this feature, foldamers are useful as a framework that can adopt different folded structures according to external stimuli such as a pH change.[2] In particular, foldamers having two or more states can act as a multiple switching molecule.[2,3]

To construct such self-organizing molecules, metal coordination bonds are frequently used. This is because coordination bonds are relatively strong among the noncovalent interactions, and their well-defined coordination geometry is useful for making the higher-order structure. Indeed, there are a number of reports on supramolecular structures, such as metallohelicates[4] and metallofoldamers,[5] based on metal-coordination bonds. We have investigated the synthesis and functions of the single-helical metal complexes that are obtained by the metal complexation of flexible oligooxime ligand **1** having two N_2O_2 coordination sites, "salamo", for d-block transition metal ions (Scheme 1a).[6−8] The exclusive formation of the single helical complex is mainly due to the fixed orientation of the two neighboring salamo sites sharing one benzene ring. We designed a new bis(N_2O_2) ligand **2** in which the two salamo sites are connected with a diethyleneoxy linker (Scheme 1b). The conformational flexibility of the linker allows the molecule to adopt a variety of higher-order folded structures. Coordination of the ethyleneoxy group to hard metal cations can change their folded structures according to the ionic radius and charge of the hard metal cations. Dynamic structural conversion between two or more folded structures would be useful to make a system that can control the functions in a multistep fashion. We now report the new diethyleneoxy-linked bis(salamo)

*To whom correspondence should be addressed. Phone: +81-29-853-4507. Fax: +81-29-853-4507. E-mail: nabesima@chem.tsukuba.ac.jp.

(1) (a) Hill, D. J.; Mio, M. J.; Prince, R. B.; Hughes, T. S.; Moore, J. S. *Chem. Rev.* **2001**, *101*, 3893–4011. (b) Huc, I. *Eur. J. Org. Chem.* **2004**, 17–29.

(2) (a) Dolain, C.; Maurizot, V.; Huc, I. *Angew. Chem., Int. Ed.* **2003**, *42*, 2738–2740. (b) Kolomiets, E.; Berl, V.; Odriozola, I.; Stadler, A.-M.; Kyritsakas, N.; Lehn, J.-M. *Chem. Commun.* **2003**, 2868–2869.

(3) Berl, V.; Huc, I.; Khoury, R. G.; Krische, M. J.; Lehn, J.-M. *Nature* **2000**, *407*, 720–723.

(4) (a) Lehn, J.-M. *Supramolecular Chemistry, Concepts and Perspectives*; Wiley-VCH: Weinheim, 1995. (b) Piguet, C.; Bernardinelli, G.; Hopfgartner, G. *Chem. Rev.* **1997**, *97*, 2005–2062.

(5) Metallofoldamers based on salen-type coordination sites, see: (a) Kawamoto, T.; Hammes, B. S.; Haggerty, B.; Yap, G. P. A.; Rheingold, A. L.; Borovik, A. S. *J. Am. Chem. Soc.* **1996**, *118*, 285–286. (b) Zhang, F.; Bai, S.; Yap, G. P. A.; Tarwade, V.; Fox, J. M. *J. Am. Chem. Soc.* **2005**, *127*, 10590–10599. (c) Dong, Z.; Karpowicz, R. J., Jr.; Bai, S.; Yap, G. P. A.; Fox, J. M. *J. Am. Chem. Soc.* **2006**, *128*, 14242–14243. (d) Wiznycia, A. V.; Desper, J.; Levy, C. J. *Inorg. Chem.* **2006**, *45*, 10034–10036. (e) Dong, Z.; Yap, G. P. A.; Fox, J. M. *J. Am. Chem. Soc.* **2007**, *129*, 11850–11853.

(6) (a) Akine, S.; Taniguchi, T.; Nabeshima, T. *Angew. Chem., Int. Ed.* **2002**, *41*, 4670–4673. (b) Akine, S.; Taniguchi, T.; Saiki, T.; Nabeshima, T. *J. Am. Chem. Soc.* **2005**, *127*, 540–541. (c) Akine, S.; Matsumoto, T.; Taniguchi, T.; Nabeshima, T. *Inorg. Chem.* **2005**, *44*, 3270–3274. (d) Akine, S.; Taniguchi, T.; Nabeshima, T. *Tetrahedron Lett.* **2006**, *47*, 8419–8422. (e) Akine, S.; Taniguchi, T.; Nabeshima, T. *J. Am. Chem. Soc.* **2006**, *128*, 15765–15774. (f) Akine, S.; Taniguchi, T.; Matsumoto, T.; Nabeshima, T. *Chem. Commun.* **2006**, 4961–4963. (g) Akine, S.; Kagiyama, S.; Nabeshima, T. *Inorg. Chem.* **2007**, *46*, 9525–9527. (h) Akine, S.; Matsumoto, T.; Nabeshima, T. *Chem. Commun.* **2008**, 4604–4606.

(7) H_2salamo = 1,2-bis(salicylideneaminooxy)ethane, see: (a) Akine, S.; Taniguchi, T.; Nabeshima, T. *Chem. Lett.* **2001**, 682–683. (b) Akine, S.; Taniguchi, T.; Dong, W.; Masubuchi, S.; Nabeshima, T. *J. Org. Chem.* **2005**, *70*, 1704–1711.

(8) (a) Akine, S.; Taniguchi, T.; Nabeshima, T. *Inorg. Chem.* **2004**, *43*, 6142–6144. (b) Akine, S.; Nabeshima, T. *Inorg. Chem.* **2005**, *44*, 1205–1207. (c) Akine, S.; Taniguchi, T.; Nabeshima, T. *Chem. Lett.* **2006**, *35*, 604–605. (d) Akine, S.; Dong, W.; Nabeshima, T. *Inorg. Chem.* **2006**, *45*, 4677–4684. (e) Akine, S.; Akimoto, A.; Shiga, T.; Oshio, H.; Nabeshima, T. *Inorg. Chem.* **2008**, *47*, 875–885.

Published on Web 10/12/2009

Scheme 1. Design of an Acyclic Ligand That Can Afford Four Kinds of Folded Structures upon Metalation

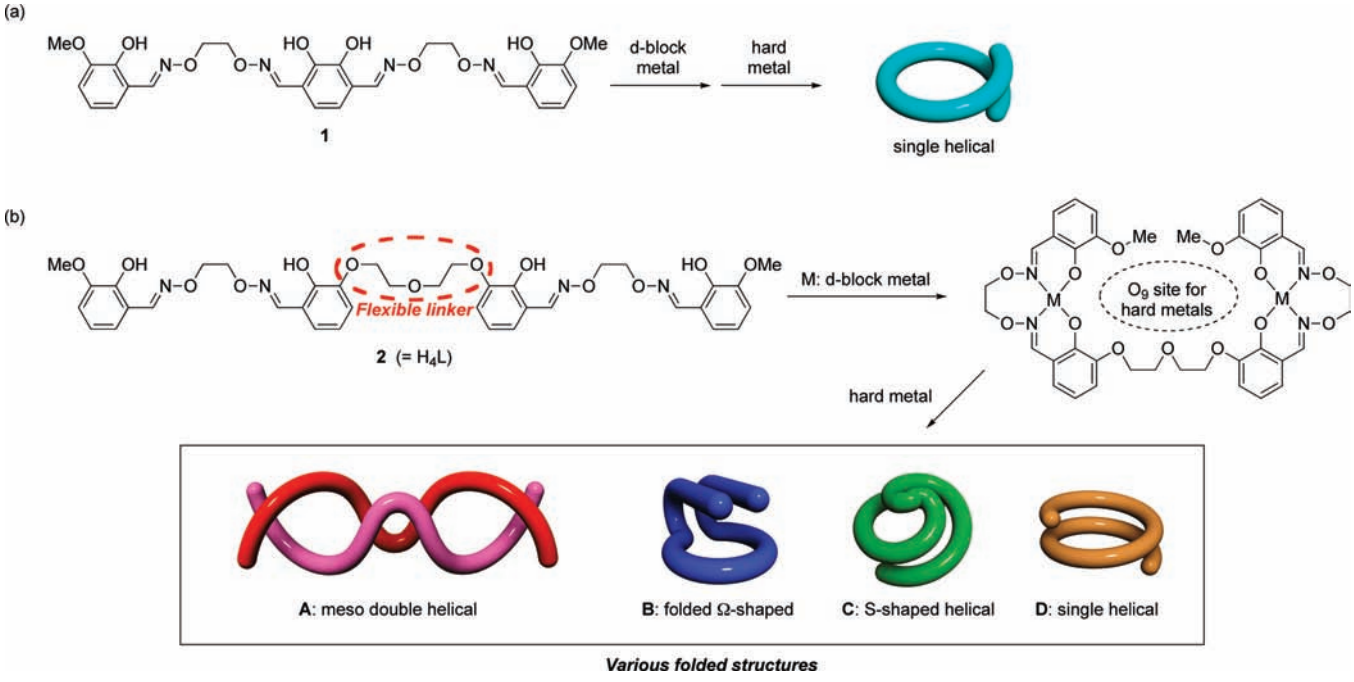

ligand **2** that can form four kinds of higher-order structures depending on the metal ions.

Experimental Section

General Procedures. All experiments were carried out in air. Commercial chloroform, methanol, and ethanol were used without purification. All chemicals were of reagent grade and were used as received. ^{1}H and ^{13}C NMR spectra were recorded on a Bruker ARX400 spectrometer (400 and 100 MHz). 2D COSY and ROESY spectra were recorded on a Bruker AV600 spectrometer (600 MHz). Mass spectra were recorded on an Applied Biosystems QStar Pulsar *i* spectrometer.

Synthesis of Ligand 2 (H_4L). A solution of 2-hydroxy-3-methoxybenzaldehyde *O*-2-(aminooxy)ethyl oxime (**3**)[7b] (453 mg, 2.00 mmol) and 3,3′-(2,2′-oxybis(ethane-2,1-diyl)bis(oxy))bis(2-hydroxybenzaldehyde) (**4**)[9] (346 mg, 1.00 mmol) in ethanol/chloroform (9:1, 15 mL) was heated at 60 °C for 2 h. After the solution was cooled to room temperature, the white precipitates were collected by filtration. The crude product was recrystallized from chloroform/hexane to give **2** (H_4L) (687 mg, 90%) as colorless crystals, mp 121−122 °C, ^{1}H NMR (400 MHz, $CDCl_3$) δ 3.90 (s, 6H), 3.97−3.99 (m, 4H), 4.22−4.24 (m, 4H), 4.47 (s, 8H), 6.79−6.97 (m, 12H), 8.25 (s, 2H), 8.27 (s, 2H), 9.60 (s, 2H), 9.73 (s, 2H). ^{13}C NMR (100 MHz, $CDCl_3$) δ 56.18 (CH_3), 69.05 (CH_2), 69.97 (CH_2), 72.89 (CH_2), 73.02 (CH_2), 113.47 (CH), 116.28 (CH), 116.47 (C), 117.01 (C), 119.43 (CH), 119.48 (CH), 122.42 (CH), 122.86 (CH), 147.09 (C), 147.15 (C), 147.63 (C), 148.16 (C), 151.39 (CH), 152.01 (CH). ESI-MS observed *m*/*z* 763.3 ($[H_4L + H]^+$), 785.3 ($[H_4L + Na]^+$). Anal. Calcd for $C_{38}H_{42}N_4O_{13}$: C, 59.84; H, 5.55; N, 7.35. Found: C, 59.60; H, 5.64; N, 7.04.

Synthesis of $[L_2Zn_6(OAc)_4]$. A solution of zinc(II) acetate dihydrate (32.8 mg, 0.15 mmol) in methanol (1 mL) was added to a solution of ligand H_4L (38.1 mg, 0.050 mmol) in chloroform (1 mL) at room temperature. Vapor phase diffusion of diethyl ether into the solution afforded pale yellow crystals of $[L_2Zn_6(OAc)_4]$ (35.2 mg, 63%). The ^{1}H NMR spectrum in $CDCl_3/CD_3OD$ (1:1) was broad and complicated (Figure S1). ESI-MS observed *m*/*z* 477.0 ($[LZn_3]^{2+}$), 1013.0 ($[LZn_3(OAc)]^+$), 2085.0 ($[L_2Zn_6(OAc)_3]^+$). Anal. Calcd for $C_{84}H_{98}N_8O_{39}Zn_6$ ($L_2Zn_6(OAc)_4$•$5H_2O$): C, 45.12; H, 4.42; N, 5.01. Found: C, 45.06; H, 4.22; N, 4.75.

Synthesis of $[LZn_4M(OH)_2(OAc)_2(MeOH)_n]X$ (M = K, X = PF_6, *n* = 2; M = Rb, X = NO_3, *n* = 1). A solution of zinc(II) acetate dihydrate (17.6 mg, 0.080 mmol) and alkali metal salt MX (= KPF_6 or $RbNO_3$, 0.020 mmol) in methanol (1 mL) was added to a solution of ligand H_4L (15.3 mg, 0.020 mmol) in chloroform (1 mL). Vapor phase diffusion of diethyl ether into the solution afforded yellow crystals of $[LZn_4M(OH)_2(OAc)_2(MeOH)_n]X$.

$[LZn_4K(OH)_2(OAc)_2(MeOH)_2]PF_6$. yield 21.5 mg, 73%. Anal. Calcd for $C_{44}H_{60}F_6KN_4O_{24}PZn_4$ ($LZn_4K(OH)_2(OAc)_2(PF_6)$•2MeOH•$3H_2O$): C, 35.84; H, 4.10; N, 3.80. Found: C, 35.29; H, 3.68; N, 3.73.

$[LZn_4Rb(OH)_2(OAc)_2(MeOH)]NO_3$. yield 17.7 mg, 57%. Anal. Calcd for $C_{45}H_{61}Cl_3N_5O_{27}RbZn_4$ ($LZn_4Rb(OH)_2(OAc)_2(NO_3)$•2MeOH•$CHCl_3$•$3H_2O$): C, 34.70; H, 3.95; N, 4.50. Found: C, 34.48; H, 4.11; N, 4.63.

Synthesis of $[LZn_2M(OAc)_2]$ (M = Ca, Sr, Ba). A solution of zinc(II) acetate dihydrate (8.8 mg, 0.040 mmol) and alkaline earth metal acetate ($M(OAc)_2$•nH_2O, 0.020 mmol) in methanol (1 mL) containing a small amount of water was added to a solution of ligand H_4L (15.3 mg, 0.020 mmol) in chloroform (1 mL) at room temperature, and the solvent was removed under reduced pressure. Vapor phase diffusion of diethyl ether into a solution of the residue in chloroform/methanol afforded yellow crystals of $[LZn_2M(OAc)_2]$.

$[LZn_2Ca(OAc)_2]$. yield 16.4 mg, 76%. ESI-MS observed *m*/*z* 465.0 ($[LZn_2Ca]^{2+}$), 959.1 ($[LZn_2Ca(OMe)]^+$), 989.1 ($[LZn_2Ca(OAc)]^+$). ^{1}H NMR (400 MHz, $CDCl_3/CD_3OD$ (1:1)) δ 1.92 (s, 6H), 3.42 (s, 6H), 3.55 (br, 2H), 3.85 (br, 2H), 4.01 (br, 2H), 4.16−4.33 (brm, 6H), 4.54 (br, 2H), 4.99 (br, 2H), 6.46 (t, *J* = 7.8 Hz, 2H), 6.53 (t, *J* = 7.8 Hz, 2H), 6.54 (br, 2H), 6.70 (d, *J* = 7.8 Hz, 2H), 6.92 (d, *J* = 7.8 Hz, 2H), 6.93 (d, *J* = 7.8 Hz, 2H), 8.36 (s, 2H), 8.49 (s, 2H). Anal. Calcd for $C_{43}H_{48}CaN_4O_{18}Zn_2$ ($LZn_2Ca(OAc)_2$•MeOH): C, 47.83; H, 4.48; N, 5.19. Found: C, 47.55; H, 4.36; N, 5.23.

(9) Van Veggel, F. C. J. M.; Bos, M.; Harkema, S.; van de Bovenkamp, H.; Verboom, W.; Reedijk, J.; Reinhoudt, D. N. *J. Org. Chem.* **1991**, *56*, 225–235.

Table 1. Crystallographic Data

compound	$[L_2Zn_6(OAc)_4]\bullet 2MeOH$	$[LZn_4K(OH)_2(OAc)_2(MeOH)_2]PF_6\bullet MeOH\bullet H_2O$	$[LZn_4Rb(OH)_2(OAc)_2(MeOH)]NO_3\bullet 1.5MeOH\bullet CHCl_3\bullet 2H_2O$	$[LZn_2Ca(OAc)_2]\bullet MeOH$	$[LZn_2Sr(OAc)_2]\bullet MeOH\bullet 0.5Et_2O$	$[LZn_2Ba(OAc)_2]\bullet H_2O\bullet 0.5Et_2O$	$[LPd_2Ba(OAc)]OAc\bullet 0.5CHCl_3\bullet H_2O$
formula	$C_{86}H_{96}N_8O_{36}Zn_6$ (2209.93)	$C_{45}H_{60}F_6KN_4O_{23}PZn_4$ (1470.52)	$C_{45.5}H_{61}Cl_3N_5O_{26.5}RbZn_4$ (1555.29)	$C_{43}H_{48}CaN_4O_{18}Zn_2$ (1079.67)	$C_{45}H_{53}N_4O_{18.5}SrZn_2$ (1164.27)	$C_{44}H_{51}BaN_4O_{18.5}Zn_2$ (1199.97)	$C_{42.5}H_{46.5}BaCl_{1.5}N_4O_{18}Pd_2$ (1304.65)
crystal system	triclinic	triclinic	monoclinic	monoclinic	triclinic	triclinic	monoclinic
space group	$P\bar{1}$	$P\bar{1}$	$P2_1/n$	$P2_1/c$	$P\bar{1}$	$P\bar{1}$	$P2_1/c$
a/Å	9.595(3)	11.4878(4)	11.4322(8)	12.5573(5)	10.030(4)	12.166(5)	16.0295(8)
b/Å	12.418(3)	16.0339(6)	25.9054(16)	69.384(3)	11.484(4)	13.771(6)	16.3410(8)
c/Å	18.678(6)	16.8551(7)	20.3002(13)	15.9265(9)	22.582(7)	14.903(8)	21.5732(14)
α/deg	92.155(11)	74.5906(12)			87.058(12)	74.24(2)	
β/deg	96.393(12)	71.3166(10)	97.739(2)	105.7057(18)	78.536(13)	89.487(18)	114.4090(10)
γ/deg	90.151(10)	76.3321(12)			70.866(14)	77.833(16)	
V/Å^3	2210.1(12)	2796.17(18)	5957.3(7)	13358.3(11)	2408.1(14)	2345.9(19)	5145.8(5)
Z	1	2	4	12	2	2	4
T/K	120	120	120	120	120	120	100
D_{calcd}/g cm^{-3}	1.660	1.747	1.734	1.611	1.606	1.699	1.684
μ/mm^{-1} (Mo Kα)	1.698	1.902	2.625	1.275	2.172	1.926	1.599
reflection collected	17673	26556	45679	103380	22689	19294	23990
unique reflections	7761	12175	10477	23200	10297	8711	9024
$2\theta_{max}$	50.00	54.00	50.00	50.00	54.00	51.00	50.00
restraints/ parameters	36/619	39/818	12/834	6/1843	0/636	16/659	108/686
GOF (F^2)	0.992	1.050	1.077	1.095	1.042	1.023	1.082
$R1^a$ ($I > 2\sigma(I)$)	0.1094	0.0436	0.0864	0.0918	0.0416	0.0698	0.0702
$wR2^a$ (all data)	0.2512	0.1199	0.2374	0.2924	0.1058	0.1783	0.2074

compound	$[LZn_2La(OAc)_2]PF_6\bullet 1.5Et_2O\bullet 0.25H_2O$	$[LZn_2Ce(OAc)_2]PF_6\bullet 1.5Et_2O\bullet 0.25H_2O$	$[LZn_2Pr(OAc)_2]PF_6\bullet 1.5Et_2O\bullet 0.25H_2O$	$[LZn_2Nd(OAc)_2]PF_6\bullet 1.5Et_2O\bullet 0.25H_2O$	$[LZn_2Sm(OAc)_2]PF_6\bullet 1.5Et_2O\bullet 0.25H_2O$	$[LZn_2Eu(OAc)_2]PF_6\bullet 1.5Et_2O\bullet 0.25H_2O$	$[LZn_2Gd(OAc)_2]PF_6\bullet 1.5Et_2O\bullet 0.25H_2O$
formula	$C_{48}H_{59.5}F_6LaN_4O_{18.75}PZn_2$ (1407.12)	$C_{48}H_{59.5}CeF_6N_4O_{18.75}PZn_2$ (1408.33)	$C_{48}H_{59.5}F_6N_4O_{18.75}PPrZn_2$ (1409.12)	$C_{48}H_{59.5}F_6N_4NdO_{18.75}PZn_2$ (1412.45)	$C_{48}H_{59.5}F_6N_4O_{18.75}PSmZn_2$ (1418.56)	$C_{48}H_{59.5}EuF_6N_4O_{18.75}PZn_2$ (1420.17)	$C_{48}H_{59.5}F_6GdN_4O_{18.75}PZn_2$ (1425.46)
crystal system	tetragonal	tetragonal	tetragonal	tetragonal	tetragonal	tetragonal	tetragonal
space group	$I4_1/a$	$I4_1/a$	$I4_1/a$	$I4_1/a$	$I4_1/a$	$I4_1/a$	$I4_1/a$
a/Å	21.226(2)	21.204(3)	21.181(2)	21.163(3)	21.136(3)	21.154(2)	21.1689(18)
c/Å	49.463(5)	49.387(6)	49.273(5)	49.188(5)	49.005(4)	48.989(6)	48.970(5)
V/Å^3	22285(4)	22204(5)	22105(4)	22029(5)	21893(4)	21923(4)	21944(3)
Z	16	16	16	16	16	16	16
T/K	120	120	120	120	120	120	120
D_{calcd}/g cm^{-3}	1.678	1.685	1.694	1.704	1.722	1.721	1.726
μ/mm^{-1} (Mo Kα)	1.731	1.788	1.854	1.919	2.055	2.125	2.188
reflection collected	105750	97929	103620	100687	104305	102941	102334
unique reflections	12150	12099	12045	12013	11932	11952	11968
$2\theta_{max}$	54.00	54.00	54.00	54.00	54.00	54.00	54.00
restraints/ parameters	24/772	25/771	24/772	25/771	24/772	24/772	24/771
GOF (F^2)	1.059	1.050	1.057	1.084	1.087	1.060	1.039
$R1^a$ ($I > 2\sigma(I)$)	0.0405	0.0441	0.0381	0.0433	0.0408	0.0434	0.0361
$wR2^a$ (all data)	0.1144	0.1166	0.1028	0.1134	0.1087	0.1051	0.1013

[a] $R1 = \Sigma||F_o| - |F_c||/\Sigma|F_o|$; $wR2 = [\Sigma(w(F_o^2 - F_c^2)^2)/\Sigma(w(F_o^2)^2)]^{1/2}$.

[$LZn_2Sr(OAc)_2$]. yield 17.8 mg, 78%. ESI-MS observed *m*/*z* 488.0 ($[LZn_2Sr]^{2+}$), 1007.0 ($[LZn_2Sr(OMe)]^+$), 1035.0 ($[LZn_2Sr(OAc)]^+$). The ^{1}H NMR spectrum in $CDCl_3/CD_3OD$ (1:1) was considerably broad (Figure S2). Anal. Calcd for $C_{43}H_{50}N_4O_{19}SrZn_2$ ($LZn_2Sr(OAc)_2$•MeOH•H_2O): C, 45.09; H, 4.40; N, 4.89. Found: C, 45.05; H, 4.35; N, 4.65.

[$LZn_2Ba(OAc)_2$]. yield 18.3 mg, 76%. ESI-MS observed *m*/*z* 513.0 ($[LZn_2Ba]^{2+}$), 1085.0 ($[LZn_2Ba(OAc)]^+$). ^{1}H NMR (400 MHz, $CDCl_3/CD_3OD$ (1:1)) δ 1.99 (s, 6H), 3.17 (brs, 6H), 3.76 (br, 8H), 4.20 (br, 4H), 4.33 (br, 4H), 6.45−6.56 (m, 8H), 6.70−6.81 (m, 4H), 8.32 (s, 2H), 8.46 (s, 2H). Anal. Calcd for $C_{44}H_{51}BaN_4O_{18.5}Zn_2$ ($LZn_2Ba(OAc)_2$•0.5Et_2O•H_2O): C, 44.04; H, 4.28; N, 4.67. Found: C, 44.09; H, 4.26; N, 4.53.

Synthesis of [$LZn_2Ln(OAc)_2$]PF_6 (Ln = La, Ce, Pr, Nd, Sm, Eu, Gd). A solution of zinc(II) acetate dihydrate (8.8 mg, 0.040 mmol), rare earth metal acetate ($Ln(OAc)_3$•*n*H_2O, 0.020 mmol), and tetrabutylammonium hexafluorophosphate (7.7 mg, 0.020 mmol) in methanol (1 mL) containing a small amount of water was added to a solution of ligand H_4L (15.3 mg, 0.020 mmol) in chloroform (1 mL) at room temperature, and the solvent was removed under reduced pressure. Vapor phase diffusion of diethyl ether into a solution of the residue in chloroform/methanol afforded pale yellow crystals of [$LZn_2Ln(OAc)_2$]PF_6.

[$LZn_2La(OAc)_2$]PF_6. yield 22.4 mg, 84%. ^{1}H NMR (400 MHz, CD_3CN) δ 2.01 (s, 6H), 3.14 (s, 6H), 3.25 (ddd, *J* = 14.0, 2.9, 2.7 Hz, 2H), 3.52 (ddd, *J* = 14.0, 9.6, 2.7 Hz, 2H), 3.64 (dt, *J* = 13.7, 2.7 Hz, 2H), 4.18 (dd, *J* = 12.8, 2.7 Hz, 2H), 4.21 (ddd, *J* = 13.7, 9.6, 2.9 Hz, 2H), 4.33 (dd, *J* = 15.8, 4.1 Hz, 2H), 4.48 (ddd, *J* = 12.8, 12.6, 4.1 Hz, 2H), 5.39 (ddd, *J* = 15.8, 12.6, 2.7 Hz, 2H), 6.35 (dd, *J* = 7.9, 1.5 Hz, 2H), 6.54 (dd, *J* = 7.8, 1.2 Hz, 2H), 6.62 (t, *J* = 7.8 Hz, 2H), 6.64 (t, *J* = 7.9 Hz, 2H), 6.97 (dd, *J* = 7.8, 1.2 Hz, 2H), 6.99 (dd, *J* = 7.9, 1.5 Hz, 2H), 8.45 (s, 2H), 8.78 (s, 2H). ESI-MS observed *m*/*z* 544.0 ($[LZn_2La(OAc)]^{2+}$), 1147.0 ($[LZn_2La(OAc)_2]^+$). Anal. Calcd for $C_{44}H_{50}F_6LaN_4O_{18}PZn_2$ ($LZn_2La(OAc)_2(PF_6)$•0.5Et_2O•0.5H_2O): C, 39.51; H, 3.77; N, 4.19. Found: C, 39.38; H, 4.06; N, 3.91.

[$LZn_2Ce(OAc)_2$]PF_6. yield 20.6 mg, 77%. ESI-MS observed *m*/*z* 343.3 ($[LZn_2Ce]^{3+}$), 543.5 ($[LZn_2Ce(OAc)]^{2+}$), 1148.0 ($[LZn_2Ce(OAc)_2]^+$). Anal. Calcd for $C_{44}H_{50}CeF_6N_4O_{18}PZn_2$ ($LZn_2Ce(OAc)_2(PF_6)$•0.5Et_2O•0.5H_2O): C, 39.47; H, 3.76; N, 4.18. Found: C, 39.19; H, 3.93; N, 3.80.

[$LZn_2Pr(OAc)_2$]PF_6. yield 20.9 mg, 77%. ESI-MS observed *m*/*z* 343.0 ($[LZn_2Pr]^{3+}$), 544.0 ($[LZn_2Pr(OAc)]^{2+}$), 1147.0 ($[LZn_2Pr(OAc)_2]^+$). Anal. Calcd for $C_{44}H_{51}F_6N_4O_{18.5}PPrZn_2$ ($LZn_2Pr(OAc)_2(PF_6)$•0.5Et_2O•H_2O): C, 39.19; H, 3.81; N, 4.15. Found: C, 38.96; H, 3.73; N, 3.89.

[$LZn_2Nd(OAc)_2$]PF_6. yield 19.6 mg, 74%. ESI-MS observed *m*/*z* 344.0 ($[LZn_2Nd]^{3+}$), 545.5 ($[LZn_2Nd(OAc)]^{2+}$), 1150.0 ($[LZn_2Nd(OAc)_2]^+$). Anal. Calcd for $C_{42}H_{48}F_6N_4NdO_{19}PZn_2$ ($LZn_2Nd(OAc)_2(PF_6)$•2H_2O): C, 37.85; H, 3.63; N, 4.20. Found: C, 37.67; H, 3.81; N, 3.84.

[$LZn_2Sm(OAc)_2$]PF_6. yield 22.5 mg, 84%. ESI-MS observed *m*/*z* 347.0 ($[LZn_2Sm]^{3+}$). Anal. Calcd for $C_{42}H_{48}F_6N_4O_{19}PSmZn_2$ ($LZn_2Sm(OAc)_2(PF_6)$•2H_2O): C, 37.67; H, 3.61; N, 4.18. Found: C, 37.68; H, 3.63; N, 3.97.

[$LZn_2Eu(OAc)_2$]PF_6. yield 16.9 mg, 62%. ESI-MS observed *m*/*z* 347.0 ($[LZn_2Eu]^{3+}$). Anal. Calcd for $C_{44}H_{51}EuF_6N_4O_{18.5}PZn_2$ ($LZn_2Eu(OAc)_2(PF_6)$•0.5Et_2O•H_2O): C, 38.87; H, 3.78; N, 4.12. Found: C, 38.43; H, 3.63; N, 3.79.

[$LZn_2Gd(OAc)_2$]PF_6. yield 18.1 mg, 66%. ESI-MS observed *m*/*z* 348.7 ($[LZn_2Gd]^{3+}$). Anal. Calcd for $C_{44}H_{51}F_6GdN_4O_{18.5}PZn_2$ ($LZn_2Gd(OAc)_2(PF_6)$•0.5Et_2O•H_2O): C, 38.72; H, 3.77; N, 4.10. Found: C, 38.38; H, 3.82; N, 3.86.

Synthesis of [$LPd_2Ba(OAc)$]OAc. Solutions of palladium(II) acetate (45.0 mg, 0.20 mmol) in chloroform (5 mL) and ligand H_4L (76.4 mg, 0.10 mmol) in chloroform (5 mL) were added to a solution of barium acetate (25.7 mg, 0.10 mmol) in methanol (10 mL) containing a small amount of water at room temperature. The solution was stirred at room temperature for 3 d and concentrated to dryness under reduced pressure. The crude product was recrystallized from chloroform/hexane to afford red crystals of [$LPd_2Ba(OAc)$]OAc (77.8 mg, 56%). ^{1}H NMR (400 MHz, $CDCl_3/CD_3OD$, (1:1)) δ 1.94 (s, 6H), 3.50 (brs, 6H), 4.21−4.34 (brm, 16H), 6.70−6.77 (m, 8H), 6.95 (d, *J* = 8.0 Hz, 2H), 7.00 (d, *J* = 7.2 Hz, 2H), 8.06 (s, 2H), 8.16 (s, 2H). ESI-MS observed *m*/*z* 555.0 ($[LPd_2Ba]^{2+}$). Anal. Calcd for $C_{42.5}H_{56.5}BaCl_{1.5}N_4O_{23}Pd_2$ ($LPd_2Ba(OAc)_2$•0.5$CHCl_3$•6H_2O): C, 36.60; H, 4.08; N, 4.02. Found: C, 36.31; H, 4.21; N, 4.07.

X-ray Crystallographic Analysis. Intensity data were collected on a Rigaku R-AXIS Rapid or a Bruker SMART APEX II diffractometer with Mo Kα radiation (λ = 0.71069 Å). Reflection data were corrected for Lorentz and Polarization factors and for absorption using the multiscan method. The structure was solved by Patterson methods (DIRDIF 99)[10] and refined by full matrix least-squares on F^2 using SHELXL 97.[11] The non-hydrogen atoms were refined anisotropically. Hydrogen atoms were included at idealized positions refined by use of the riding models except for water molecules in the crystals of [$LZn_4Rb(OH)_2(OAc)_2(MeOH)$]$NO_3$, [$LZn_2Ln(OAc)_2$]$PF_6$, and [$LPd_2Ba(OAc)$]OAc. The crystallographic data are summarized in Table 1.

Optical Measurements. UV−vis absorption spectra were recorded in a 10-mm-path-length quartz cell on a JASCO V-660 spectrophotometer. Visible/near-infrared emission spectra in a range of 350−1100 nm were recorded on a Hamamatsu Photonics PMA-12 Multichannel Analyzer using an air-equilibrated solution of complexes (0.02 mM) in acetonitrile with an excitation wavelength of 350 nm. The absolute quantum yield of [$LZn_2La(OAc)_2$]PF_6 was determined using an integration sphere equipped with a Hamamatsu Photonics PMA-12 Multichannel Analyzer.

Results and Discussion

Design and Synthesis of Ligand 2. For designing the ligand, the diethyleneoxy group was used as the flexible linker, which locates between the two N_2O_2 salamo units. The oxime-based salamo ligand is useful for constructing the acyclic oligo(N_2O_2) structure because the oxime C=N bonds are more stable against the recombination than the imine C=N bonds. The ligand **2** was synthesized in 90% yield by the reaction of 2-hydroxy-3-methoxybenzaldehyde *O*-2-(aminooxy)ethyl oxime (**3**)[7b] with 3,3′-(2,2′-oxybis(ethane-2,1-diyl)bis(oxy))bis(2-hydroxybenzaldehyde) (**4**)[9] in chloroform/ethanol (Scheme 2).

Scheme 2. Synthesis of Ligand **2**

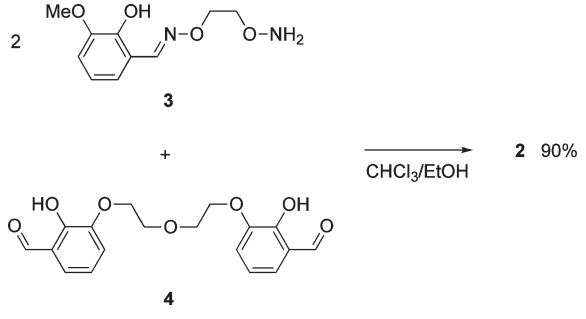

(10) Beurskens, P. T.; Beurskens, G.; de Gelder, R.; Garcia-Granda, S.; Gould, R. O.; Israel R.; Smits, J. M. M. *The DIRDIF 99 program system*; Crystallography Laboratory, University of Nijmegen: Nijmegen, The Netherlands, 1999.

(11) Sheldrick, G. M. *SHELXL 97, Program for crystal structure refinement*; University of Göttingen: Göttingen, Germany, 1997.

The two N_2O_2 salamo sites of the ligand **2** are expected to coordinate to softer d-block transition metals in a tetradentate fashion.[7a,8] The phenoxo oxygen atoms of the resultant N_2O_2-complex can further coordinate to a harder cation through the μ-phenoxo bridge. In addition, the ether oxygen atoms of the linker have a coordination ability to a hard metal cation, which would affect the higher-order folded structure of the ligand **2** according to the nature of the hard cations.

Formation of Meso Double Helical Structure by Complexation with Zinc(II). The complexation of the ligand **2** (= H_4L) with zinc(II) acetate produced a crystalline complex having the ligand and zinc(II) in a 1:3 stoichiometry. The pale yellow crystals were isolated in 63% yield. An X-ray crystallographic analysis revealed the dimeric structure of the hexanuclear complex $[L_2Zn_6(OAc)_4]$ (Figure 1). The complex has two zinc(II) trinuclear cores, in which the two salamo moieties are provided by one ligand L and the other. The structural feature around the zinc atoms in the $(salamo)_2Zn_3$ units is quite similar to that of the mono(salamo) analog $[(3\text{-MeOsalamo})_2Zn_3(OAc)_2]$.[8a] Since the two $(salamo)_2Zn_3$ cores are related by a crystallographically imposed inversion center, the molecule has an achiral meso double helical structure. The geometry around the central zinc (Zn2) is distorted octahedral, whereas Zn1 and Zn3 are in a distorted trigonal bipyramidal environment. In solution, however, the hexanuclear complex $[L_2Zn_6(OAc)_4]$ partly dissociates to give a mixture of complexes. The ^1H NMR spectrum in $CDCl_3/CD_3OD$ (1:1) was significantly broad and complicated (Figure S1). The ESI mass spectrum of the solution exhibited intense peaks at m/z 477.0 for $[LZn_3]^{2+}$ and m/z 1013.0 for $[LZn_3(OAc)]^+$ in addition to a weak peak at m/z 2085.0 corresponding to the hexanuclear species of $[L_2Zn_6(OAc)_3]^+$. These results strongly indicate that the hexanuclear complex remains in solution, but the complex is significantly dissociated into the trinuclear complex.

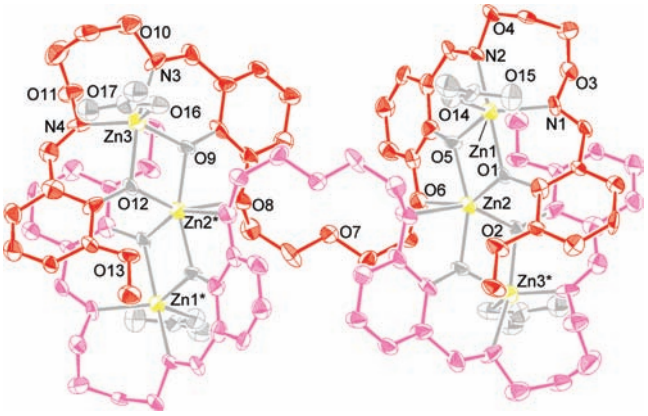

Figure 1. Crystal structure of hexanuclear complex $[L_2Zn_6(OAc)_4]$ with thermal ellipsoids drawn at 30% probability level.

Formation of Folded Ω-Shaped Structure by Complexation with Zinc(II) and Alkali Metal Cation. When the complexation with zinc(II) was carried out in the presence of an alkali metal cation (K^+ or Rb^+), a monomeric heterometal complex was obtained. An X-ray crystallographic analysis of the complex revealed the structure of the pentanuclear complex $[LZn_4M(OH)_2(OAc)_2(MeOH)_n]X$ (M = K, X = PF_6, n = 2; M = Rb, X = NO_3, n = 1) (Figure 2). Each of the salamo sites coordinates to zinc (Zn1, Zn2) in an N_2O_2 tetradentate fashion, which further coordinates to another zinc (Zn3, Zn4) in a bridging fashion. The salamoZn_2 moieties are doubly bridged by two hydroxo groups (O14, O15), thus making a Zn_4 cluster moiety. Furthermore, five oxygen donor atoms (three ether oxygen atoms (O6, O7, O8) and two phenoxo groups (O5, O9)) are cyclically arrayed to form a binding site for a K^+ or Rb^+ ion. In these complexes, the ligand moiety adopts a folded Ω-shaped conformation in which two terminal benzene rings are stacked on top of each other at a distance of 3.4 Å. This Ω-shaped conformation probably results from the π-stacking interaction as well as the multiple coordination bonds in the

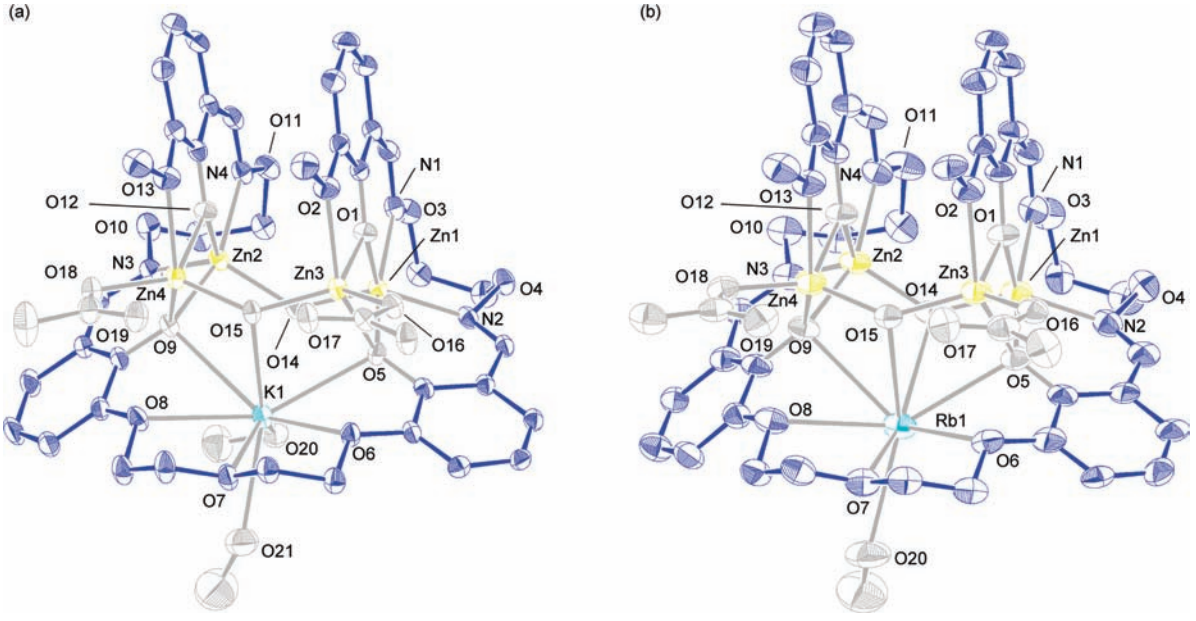

Figure 2. Crystal structure of pentanuclear complexes (a) $[LZn_4K(OH)_2(OAc)_2(MeOH)_2]PF_6$ and (b) $[LZn_4Rb(OH)_2(OAc)_2(MeOH)]NO_3$ with thermal ellipsoids drawn at 50% probability level. Hydrogen atoms and counteranions are omitted for clarity.

pentanuclear Zn_4K or Zn_4Rb core. The ESI mass spectra of the solution showed peaks attributed to $[LZn_2]$, while no peak corresponding to the pentanuclear species was observed. This result suggested the dissociation of the pentanuclear complex $[LZn_4M(OH)_2(OAc)_2]^+$ (M = K or Rb) in solution.

Formation of S-Shaped Helical Structure by Complexation with Zinc(II) and Alkaline Earth or Rare Earth Metal Cation. The complexation of the ligand **2** with zinc(II) and alkaline earth metal ions afforded the trinuclear complex $[LZn_2M(OAc)_2]$ (M = Ca, Sr, Ba). The crystal structures were determined by X-ray crystallography (Figure 3a−c). The two salamo-Zn^{2+} moieties intersect each other and simultaneously coordinate to one alkaline earth metal ion (Ca^{2+}, Sr^{2+}, Ba^{2+}). The ligand moiety makes an S-shaped helical structure in which the two salamo arms are helically radiated from the diethyleneoxy bridge. Two acetato ligands coordinate from the opposite side of the diethyleneoxy bridge to the Zn-M-Zn core in a μ-bridging fashion. In these complexes, all the phenoxo (O1, O5, O9, O12) and four aromatic ether oxygen atoms (O2, O6, O8, O13) are involved in the coordination to the alkaline earth metal ion. In the calcium complex $[LZn_2Ca(OAc)_2]$ the aliphatic ether oxygen atom (O7) of the diethyleneoxy moiety also coordinates to the calcium ion.

Complexation of the ligand **2** with zinc(II) and lanthanum(III) also produced a trinuclear complex $[LZn_2La(OAc)_2]^+$ having an S-shaped helical structure similar to $[LZn_2Ba(OAc)_2]$. The complex was isolated as a hexafluorophosphate salt, $[LZn_2La(OAc)_2]PF_6$, and the structure was determined by X-ray crystallography (Figure 3d). The ESI mass spectrum of the complex showed intense peaks at m/z 544.0 for $[LZn_2La(OAc)]^{2+}$ and m/z 1147.0 for $[LZn_2La(OAc)_2]^+$, indicating that the trinuclear structure is maintained in solution. The ^1H NMR spectrum of $[LZn_2La(OAc)_2]PF_6$ in CD_3CN showed well-resolved sharp signals (Figure 4). All the diastereotopic methylene protons (H_e, H_f, H_k, H_l) were observed as nonequivalent signals corresponding to the C_2-symmetric structure. Upfield shift of the terminal methoxy protons (observed at 3.14 ppm) implies that the methoxy groups are located in the shielding region of the aromatic rings. In addition, the 2D-ROESY spectrum showed several ROE correlations that agree with the folded structure revealed by the X-ray crystallographic analysis.

The complexation of the ligand H_4L with zinc(II) and other light lanthanide(III) ions (Ln = Ce, Pr, Nd, Sm, Eu, Gd) also produced a trinuclear complex $[LZn_2Ln(OAc)_2]PF_6$. All the crystals were isomorphous and the molecular structures were essentially the same (Figures S6−S12).

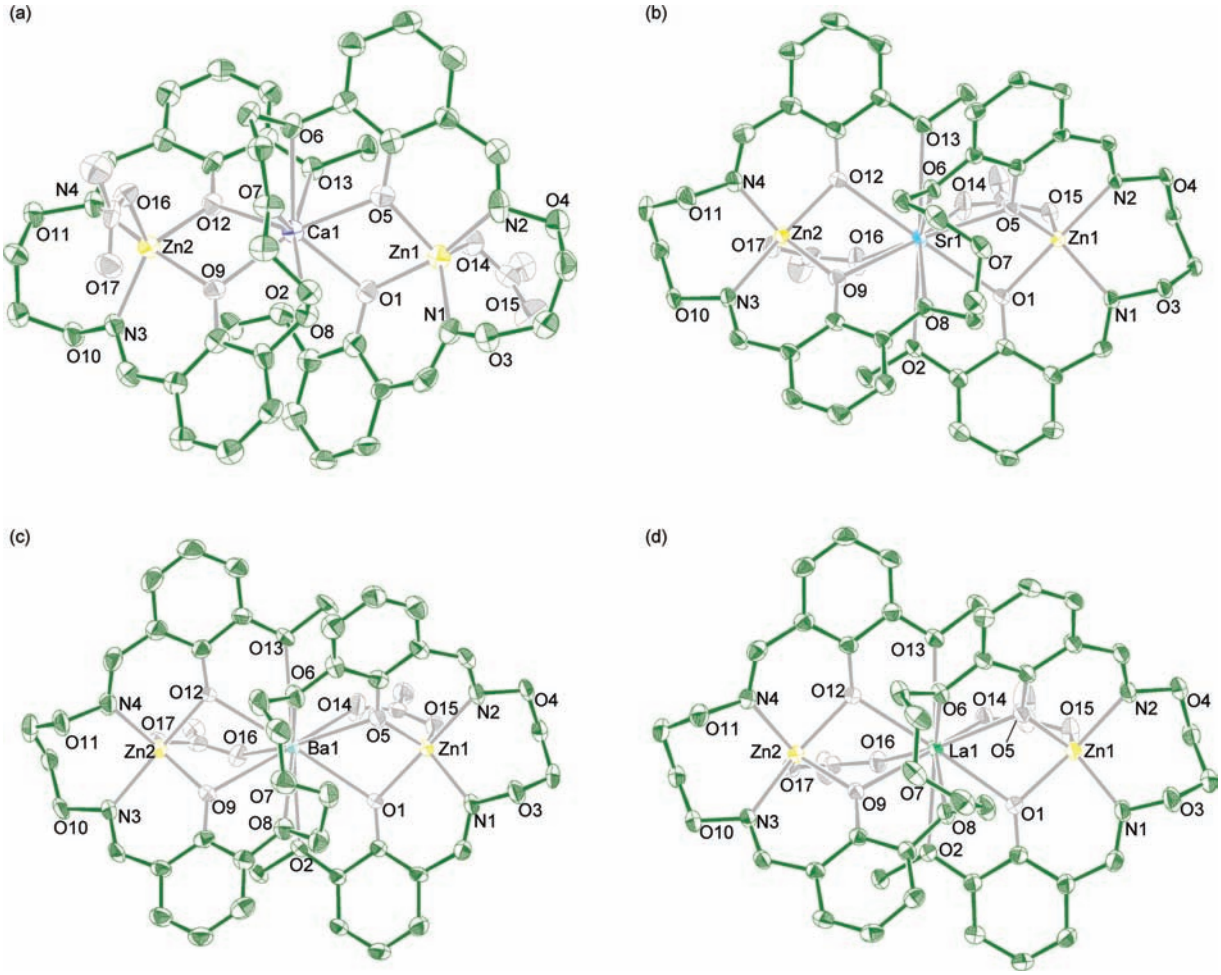

Figure 3. Crystal structures of trinuclear complexes (a) $[LZn_2Ca(OAc)_2]$; (b) $[LZn_2Sr(OAc)_2]$; (c) $[LZn_2Ba(OAc)_2]$; and (d) $[LZn_2La(OAc)_2]^+$. Thermal ellipsoids are drawn at the 50% probability level. For $[LZn_2Ca(OAc)_2]$, only one of the crystallographically independent molecules is shown.

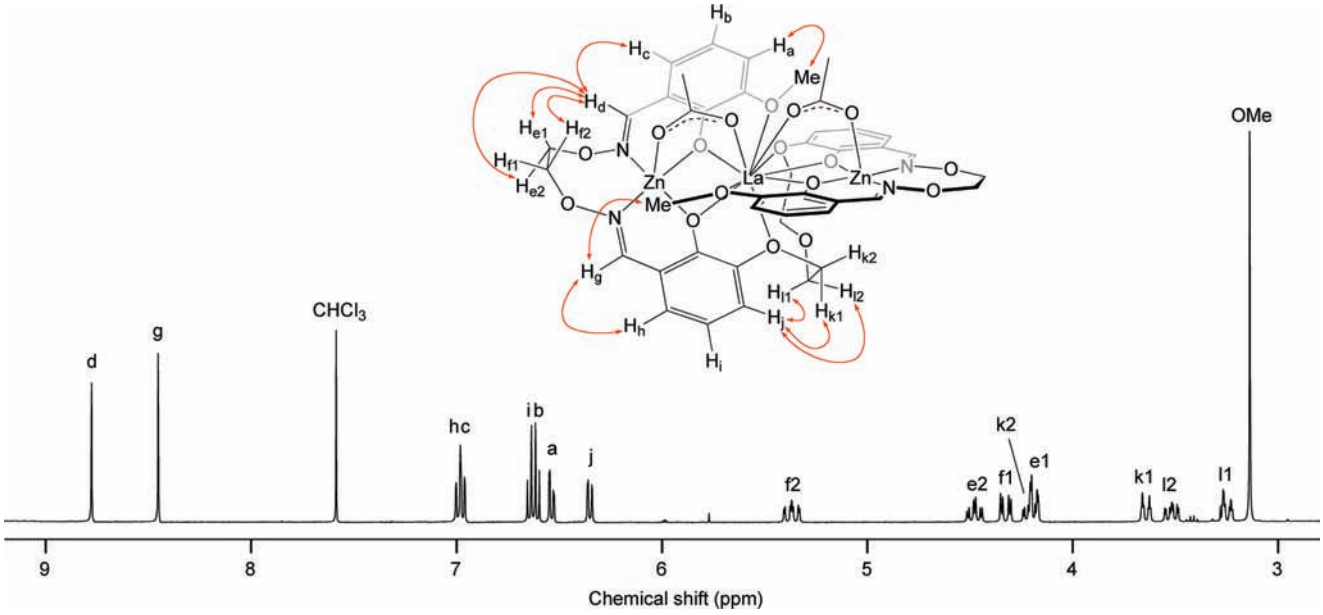

Figure 4. ^{1}H NMR spectrum of $[LZn_2La(OAc)_2]PF_6$ in CD_3CN at 400 MHz. Assignments are based on 2D-COSY and ROESY spectra. Arrows indicate the observed ROE correlations.

The lanthanum complex $[LZn_2La(OAc)_2]PF_6$ showed a relatively intense ligand-centered emission at 477 nm in an acetonitrile solution under excitation at 350 nm (Figure 5). The quantum yield was determined to be 2.3%. The luminescence spectrum of $[LZn_2Sm(OAc)_2]PF_6$ showed four narrow emission peaks at 558, 596, 642, and 700 nm, which are assigned to the typical $^4G_{5/2} \rightarrow {}^6H_J$ (J = 5/2, 7/2, 9/2, 11/2) transition of Sm^{3+} (Figure 5). A weak and broadband at around 482 nm in the spectrum can be assigned to the intraligand fluorescent emission of L^{4-}. The luminescence spectra of $[LZn_2Eu(OAc)_2]PF_6$ and $[LZn_2Pr(OAc)_2]PF_6$ also showed a visible f-f emission at 611 nm ($^5D_0 \rightarrow {}^7F_2$) and 602 nm ($^1D_2 \rightarrow {}^3H_4$), respectively. In the spectrum of $[LZn_2Nd(OAc)_2]PF_6$, the near-infrared emission in the 850−920 nm region, which is assignable to the $^4F_{3/2} \rightarrow {}^4I_{9/2}$ transition of Nd^{3+}, was observed.[12] Consequently, the trinuclear complexes $[LZn_2Ln(OAc)_2]PF_6$ (Ln = Pr, Nd, Sm, Eu) exhibit visible or near-infrared luminescence due to the f-f transition. The energy transfer from $[LZn_2]$ moiety to lanthanide(III) ion occurs efficiently. This contrasts starkly with the single helical zinc(II)-lanthanide(III) complexes obtained from ligand **1**, which do not exhibit lanthanide(III) luminescence in the visible region.[13]

Formation of Single Helical Structure by Complexation with Palladium(II) and Barium Ion. As described above, the hard metal cation significantly affects the structure of the complex by interacting with oxygen donor atoms. It is also expected that d-block metals having a different geometry produce a structure with a different folding process.

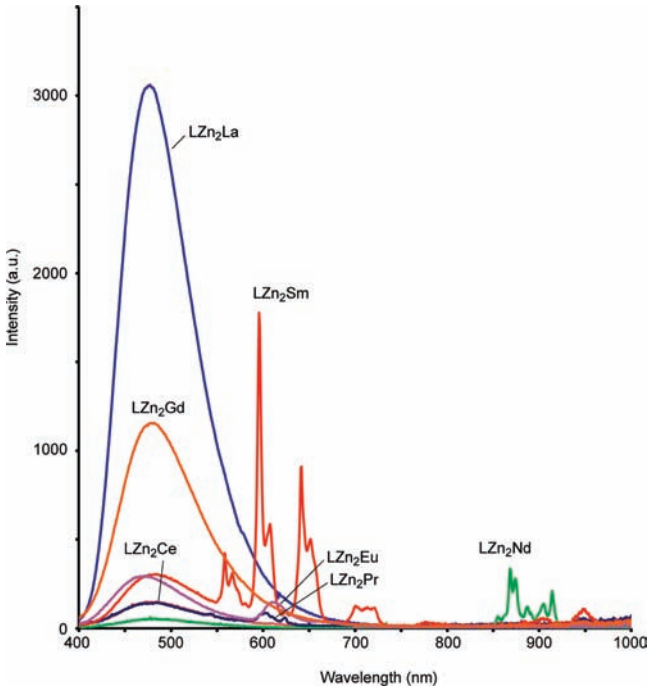

Figure 5. Luminescence spectra of $[LZn_2Ln(OAc)_2]PF_6$ recorded in 0.02 mM acetonitrile solution.

We used palladium(II) as the diamagnetic d-block metal source. The mixed metal trinuclear complex $[LPd_2Ba(OAc)]OAc$ was obtained in 56% yield by the reaction of H_4L with palladium(II) acetate and barium acetate. In the ESI-mass spectrum, an intense peak at m/z 555.0 assignable to $[LPd_2Ba]^{2+}$ clearly indicates the formation of the trinuclear structure. The ^{1}H NMR spectral pattern indicates the symmetrical structure in which two terminals are in equivalent environment.

We obtained a single crystal of $[LPd_2Ba(OAc)]OAc$ suitable for X-ray crystallography (Figure 6). The two square planar palladium atoms (Pd1, Pd2) sit in the two

(12) Several dimetallic zinc(II)-lanthanide(III) complexes with salen-type ligands emit near infrared luminescence, see: (a) Wong, W.-K.; Liang, H.; Wong, W.-Y.; Cai, Z.; Li, K.-F.; Cheah, K.-W. *New J. Chem.* **2002**, *26*, 275–278. (b) Margeat, O.; Lacroix, P. G.; Costes, J.-P.; Donnadieu, B.; Lepetit, C.; Nakatani, K. *Inorg. Chem.* **2004**, *43*, 4743–4750. (c) Lo, W.-K.; Wong, W.-K.; Guo, J.; Wong, W.-Y.; Li, K.-F.; Cheah, K.-W. *Inorg. Chim. Acta* **2004**, *357*, 4510–4521. (d) Yang, X.; Jones, R. A.; Lynch, V.; Oye, M. M.; Holmes, A. L. *Dalton Trans.* **2005**, 849–851.

(13) Akine, S.; Utsuno, F.; Nabeshima, T. *IOP Conf. Ser.: Mater. Sci. Eng.* **2009**, *1*, 012009.

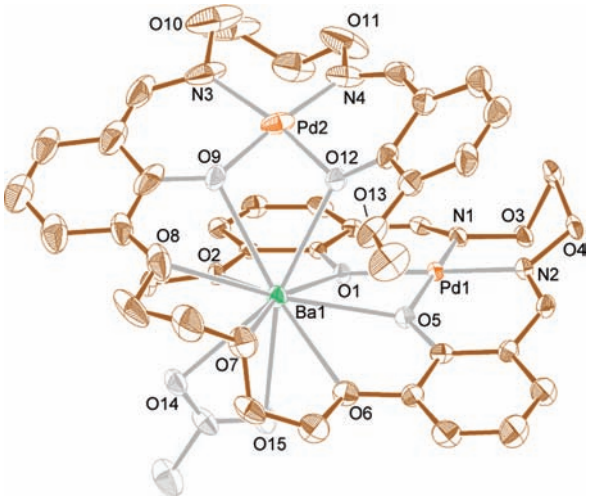

Figure 6. Crystal structure of the trinuclear complex $[LPd_2Ba(OAc)]^+$ with thermal ellipsoids drawn at the 20% probability level.

N_2O_2 salamo moieties. The nine oxygen donors coming from the methoxy (O2, O13), phenoxo (O1, O5, O9, O12), and ether oxygen atoms (O6, O7, O8) coordinate to Ba^{2+}. Thus, the ligand winds around the Ba^{2+} to make a single helix with more than one-turn (winding angle:[14] 438 deg).

Investigation of Structural Conversion between the Folded Structures. The ligand H_4L can adopt four kinds of folded conformations depending on the metal ions. If these four structures are interconvertible, the system is useful for multistep switching. Therefore, we investigated the conversion between the four kinds of structures.

While the hexanuclear complex $[L_2Zn_6(OAc)_4]$ dissociates into several species in solution, the complex is converted into a discrete species (Figure 7b,f), upon the addition of alkaline earth and rare earth metal ions (Ba^{2+} or La^{3+}). The ^1H NMR spectra indicate the formation of $[LZn_2Ba(OAc)_2]$ and $[LZn_2La(OAc)_2]^+$ (Figure 7a,e). This process corresponds to the structural conversion from the meso double helical structure into an S-shaped helical structure (Scheme 3). Similarly, conversion from the folded Ω-shaped structure to the S-shaped helical one was also observed upon the addition of Ba^{2+} or La^{3+} to a solution of $[LZn_4K(OH)_2(OAc)_2(MeOH)_2]^+$ (not shown). When 1 equiv of La^{3+} was added to $[LZn_2Ba(OAc)_2]$ or 1 equiv of Ba^{2+} was added to $[LZn_2La(OAc)_2]^+$, a mixture of $[LZn_2La(OAc)_2]^+$ and $[LZn_2Ba(OAc)_2]$ was obtained (Figure 7c,d).[15] Thus, the conversion between $[LZn_2Ba(OAc)_2]$ and $[LZn_2La(OAc)_2]^+$ is reversible. In addition, $[LZn_2Ba(OAc)_2]$ was converted into the single helical $[LPd_2Ba(OAc)]^+$ by the reaction with $Pd(OAc)_2$ (Figure 7g,h). Consequently, we achieved a two-step conversion among the three kinds of folded structures; from the meso double helical $[L_2Zn_6(OAc)_4]$ to the S-shaped helical $[LZn_2Ba(OAc)_2]$ and then to the single helical $[LPd_2Ba(OAc)]^+$ (Scheme 3).

(14) Winding angle is defined as the sum of eight O−Ba−O angles (O2−Ba1−O1, O1−Ba1−O5, O5−Ba1−O6, O6−Ba1−O7, O7−Ba1−O8, O8−Ba1−O9, O9−Ba1−O12, O9−Ba1−O13).

(15) The slight difference between the solutions (c) and (d) in the ratio of $[LZn_2Ba]^{2+}$ to $[LZn_2La]^{3+}$ in Figure 7 is probably because of the difference in counteranions; 5 mol of OAc^- for solution (c) whereas 4 mol of OAc^- and 1 mol of PF_6^- for solution (d).

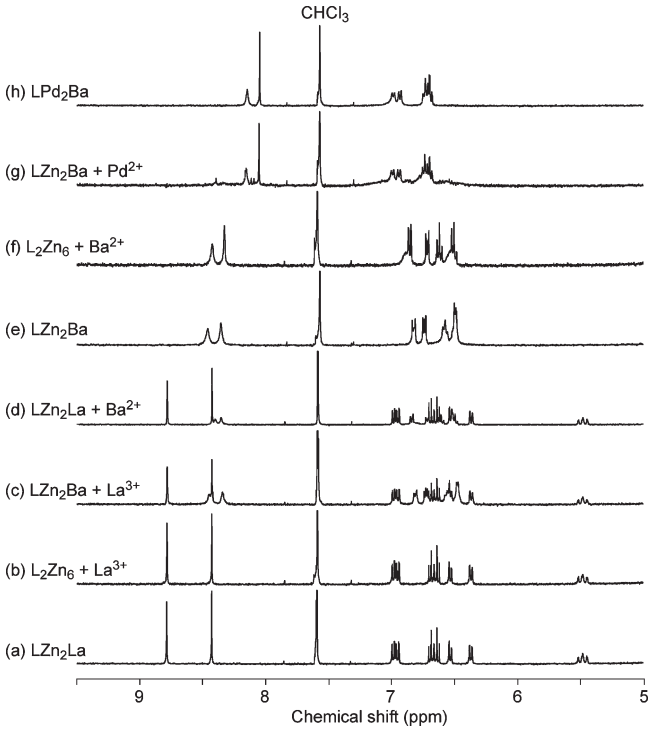

Figure 7. ^1H NMR spectra (400 MHz, $CDCl_3/CD_3OD$ (1:1)) of metal complexes ($[LZn_2La(OAc)_2]^+$, $[L_2Zn_6(OAc)_4]$, $[LZn_2Ba(OAc)_2]$, $[LPd_2Ba(OAc)]^+$) in the absence and presence of metal salt (La^{3+}, Ba^{2+} (1 equiv) or Pd^{2+} (2 equiv)).

Scheme 3. Conversion between the Various Kinds of Folded Structures[a]

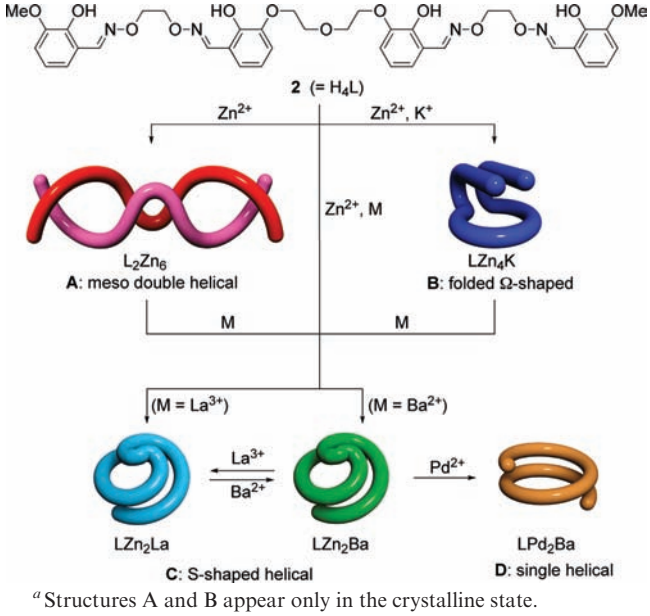

[a] Structures A and B appear only in the crystalline state.

Conclusion

Various kinds of folded structures were formed by the multimetal complexation of the flexible ligand incorporating the two types of coordination sites, the N_2O_2 salamo moiety for soft metals and the diethyleneoxy moiety for hard metals. The difference in the affinity to metal ions resulted in variation of the folding modes and enabled the structural conversion among the folded structures. Such a metal-mediated

conversion would be useful for developing a sophisticated multistep switching system that can change the physicochemical properties based on the organic framework or the oligometallic core.

Acknowledgment. We thank Dr. Kenji Yoza (Bruker AXS KK) for the X-ray crystallographic analysis data collection of $[LPd_2Ba(OAc)]OAc$. This work was supported by Grants-in-Aid for Scientific Research from the Ministry of Education, Culture, Sports, Science and Technology, Japan.

Supporting Information Available: X-ray crystallographic data in CIF format and ^1H NMR spectra ($[L_2Zn_6(OAc)_4]$ and $[LZn_2Sr(OAc)_2]$), ^1H NMR titration data for structural conversion, and crystal structure of $[LZn_2Ln(OAc)_2]^+$ (Ln = La, Ce, Pr, Nd, Sm, Eu, Gd). This material is available free of charge via the Internet at http://pubs.acs.org.